

Comparative Performance Analysis of G-RAKE Receivers with Suboptimal Finger Placement

K. B. Baltzis* and E. S. Meles

Radio Communications Laboratory, Department of Physics, Aristotle University of Thessaloniki, Thessaloniki, Greece

Received 6 June 2012; Accepted 24 July 2014

Abstract

Generalized RAKE (G-RAKE) reception reduces the total amount of interference and provides enhanced diversity by comprising extra fingers to collect information about interference and further using channel and impairment correlation estimates for fingers allocation. However, the hardware complexity and the excessive computational requirements of G-RAKE receivers may restrict their application in real systems; thus, suboptimal solutions are commonly used. In this paper, we propose and evaluate three maximum likelihood G-RAKE structures for colored noise with suboptimal finger placement. In all implementations, the fingers are optimally distributed within a time window that spans from several chip periods before the first arriving multipath to several chip periods after the latest one. The first receiver has its fingers at integer multiples of the chip period while in the rest two structures the search window is segmented in halves and tenths of the chip duration. This work also extends earlier studies by thoroughly investigating the impact of fractionally spaced finger placement on system performance. Our analysis shows that a suboptimal finger allocation reduces hardware complexity with negligible performance loss. The impact of channel delay spread and processing gain on system performance is also investigated and gives interesting results.

Keywords: G-RAKE, interference suppression, colored noise, DS-CDMA, wireless communications

2. Introduction

Wireless communications are looking nowadays for high-speed internet access and broadband services; moreover, they aim to revolutionize the way we communicate and offer a vast range of converged devices, services and networks [1]. The increasing demands for wireless multimedia and interactive internet services require the design of novel systems for high-speed, reliable and cost-effective data transmission [2]. A wireless access technology adopted in the third generation (3G) communication systems that supports variable and high data rate services and high system capacity is the (Wideband) Code Division Multiple Access ((W)-CDMA) [3,4], a digital technology that uses direct sequence spread spectrum (DS/SS) techniques [5].

In the last two decades, extensive research has been devoted for the design of highly efficient DS/SS receivers that provide a good tradeoff between performance and complexity. An attractive choice is the RAKE receiver [6] which uses baseband correlators (fingers) to individually process multipath signal components that are properly combined to improve the signal-to-noise ratio (SNR) and reduce the probability of deep fades. In conventional RAKE reception [6,7], the fingers collect resolvable signal multipaths, that is, each finger extracts the signal from a multipath component generated by the channel. Then, the received signal components are suitably combined after despreading by a local copy of the delayed version of the transmitter's spreading sequence so as to determine the

decision variable.

An advanced RAKE structure is the generalized RAKE (G-RAKE) receiver [6,8-10]. In contrast to conventional RAKE reception, the G-RAKE comprises extra fingers to collect information about interference and uses channel and impairment correlation estimates to form the combining weights not only for maximizing the received (desired) signal energy but also to suppress interference. Moreover, in the design of G-RAKES, both fingers positions and combining weights are considered. In a representative coherent G-RAKE proposal [8], the combining weights of the fingers are determined by the maximization of the decision statistic's SNR using maximum likelihood (ML) principles. In a proposed embodiment, optimum finger placement is obtained from an exhaustive search in a time window that spans from several chip periods before the first arriving multipath to several chip periods after the latest arriving one. In a second design proposal, a subset of the fingers is aligned with the incoming multipaths and the rest of them are placed on the strongest taps of the inverse channel filter. With this placement, the receiver approximates inverse channel filtering, thereby cancelling the noise coloration caused by the channel and achieving partial own-cell interference cancellation [10].

Despite the G-RAKES' enhanced performance which has led [9] to their incorporation in Ericsson's [11] HSDPA/EDGE¹ mobile platforms U350 and U360, their increased hardware complexity and computational requirements, restrict their use for real-time applications, esp.

* E-mail address: kbaltzis@auth.gr

¹ The acronyms HSDPA and EDGE stand for High-Speed Downlink Packet Access and Enhanced Data rates for GSM Evolution, respectively.

in wideband channels with large energy and delay spread. Nowadays, a major challenge for electrical and communication engineers is the development and design of suboptimal structures that significantly reduce the computational and hardware complexity of the receivers with a reasonable performance loss, e.g. [12-15].

This issue is treated herein². We present three suboptimal DS-CDMA G-RAKE receivers for colored noise with different finger placement strategies. In the first design, fingers are optimally set at integer multiples of the chip period. In the rest two implementations, fingers are optimally distributed in a time window segmented in halves and tenths of the chip duration. In all cases, the finger positions and combining weights are obtained from the maximization of the decision statistic's SNR by using ML principles as in [8]. Within this context, we further study the relation between fingers placement, bit error rate and system capacity. Finally, we investigate the impact of channel spread and processing gain on system performance for the proposed implementations. Comparisons with notable methods show the efficacy and the applicability of our proposal. The obtained results lead to interesting conclusions about the tradeoff between system performance and complexity.

The rest of the paper is organized as follows. Section 2 discusses the basic principles of generalized RAKE reception and provides the mathematical formulation for the performance evaluation of the proposed G-RAKE receivers. System model and assumptions are given in Section 3. Numerical results and discussions are presented in Section 4. Finally, Section 5 concludes the paper.

3. Theoretical Background and Mathematical Formulation

The purpose of this Section is twofold. First, it outlines the basic principles of generalized RAKE reception and describes the structure of a representative G-RAKE receiver. Then, it provides the mathematical formulation for the calculation of the bit error rate (BER) in a DS-CDMA wireless communication system that comprises a generalized RAKE at the receiver site.

3.1 Generalized RAKE reception: Basic principles and receiver structure

In the published scientific and patent literature, several G-RAKE receiver designs with different combinations of performance and complexity can be found. Here, we consider a symbol-level coherent G-RAKE receiver [8] with structure similar to the conventional maximum-ratio combining (MRC) RAKE [6,7]. In both receivers, the fingers despread the incoming signal at different time delays and their outputs are suitably combined to form symbol estimates. However, the two implementations differ in that the conventional RAKE aims to the maximization of the desired signal received energy by properly setting fingers delays and combining weights while in the G-RAKE finger placement and weight computation further targets to interference suppression. In order to do so, the G-RAKE may comprise more fingers than the number of the resolvable signal multipaths L . Besides channel estimation,

the G-RAKE receiver estimates the correlation between the interference plus noise on different fingers so as to suppress interference [9].

The structure of a typical G-RAKE receiver is given in Fig. 1. The receiver has $J \geq L$ fingers that track individual signal multipaths of the received signal $r(t)$ and correlate them to different time delays $d_j, j = 1..J$. The fingers outputs $y(d_j)$ are then multiplied with the conjugates of the combining weights w_j to form the decision statistic

$$Z = \sum_{j=1}^J w_j^* y(d_j) \tag{1}$$

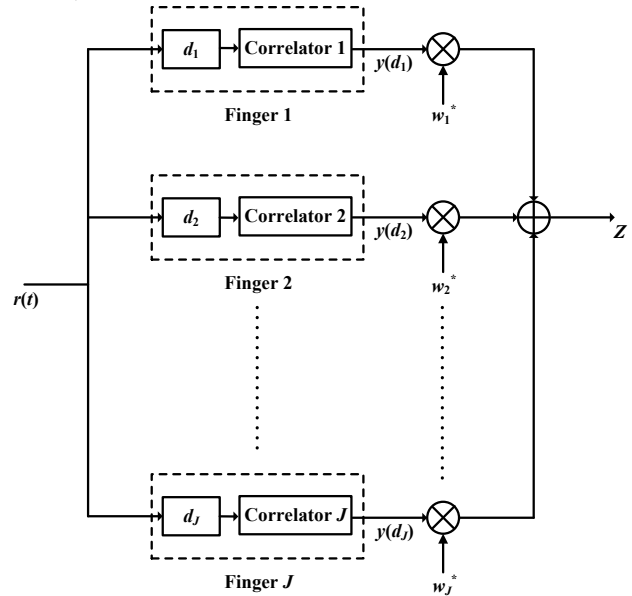


Fig. 1. J-finger G-RAKE receiver model.

In [8], the combining weights are calculated by using ML principles. Finger allocation is a tradeoff between channel matching and noise whitening. Different finger placement strategies can be employed. For example, in time-invariant channels, the maximization of SNR may determine the optimal finger delays; when the channel is time-varying, the optimization criterion is either the maximization of the instantaneous SNR or the minimization of the bit error rate. However, in any case, the optimum fingers delays d_j are found with an exhaustive search in a time window that ranges before the earliest arriving multipath component up to several chip periods after the latest arriving one. The placement of one or more extra fingers at proper positions before the first arriving multipath further approximates inverse channel filtering [17] so as to cancel noise coloration and further reduce the interference level.

3.2 Bit error rate calculation

We consider a DS-CDMA communication system with K active users. Let us set T the symbol duration, T_c the chip period, N the processing gain, that is, the ratio T to T_c , $\{c_{k,i}(j)\}_{j=0}^{N-1}$ the k th user's spreading code for the i th bit, $h(t)$ the normalized chip pulse waveform and E_k the average symbol energy of the k th user.

In the cases of BPSK or QPSK modulation, the bit error rate for coherent reception is [17]

² This work has been partially presented in the 2nd Pan-Hellenic Conference on Electronics and Communications, Thessaloniki, Greece, March 16-18, 2012 [16].

$$P_e = \frac{1}{2} \operatorname{erfc}(\sqrt{aSNR}) \quad (2)$$

where parameter a is 1 for BPSK and 0.5 for QPSK modulation while the signal-to-noise ratio SNR at the output of the combiner is equivalent to the receiver gain, that is, the ratio of the desired user (user “0”) symbol energy to the power spectral density of the overall noise.

The authors in [8] modeled the intracell interference as colored Gaussian noise to account for multipath dispersion and the intercell interference plus thermal noise as white Gaussian noise. The validity of the last assumption is further justified when the G-RAKE receives a plurality of signals; in this case, the intercell interference is approximately white and it is further colored by the pulse shape. Under these impairments modeling assumptions, the SNR in (2) may be calculated from the expression

$$SNR = \mathbf{y}_d^H \left(\mathbf{R}_S + \frac{E_I}{E_0} \mathbf{R}_M + \frac{N_0}{E_0} \mathbf{R}_N \right)^{-1} \mathbf{y}_d \quad (3)$$

where superscript H stands for the Hermitian transpose operator, notation $(\cdot)^{-1}$ denotes the inverse matrix, $E_I = \sum_{k=1}^K E_k$ is the total symbol energy of the intracell interference, N_0 is the single-sided power spectral density of the intercell interference plus thermal noise, and \mathbf{y}_d , \mathbf{R}_S , \mathbf{R}_M and \mathbf{R}_N are, respectively, the J -dimensional desired signal vector and the $J \times J$ covariance matrices of intersymbol interference (ISI), multiple user interference (MUI) and overall noise at the fingers outputs, with elements given by:

$$y_d(d_\mu) = \frac{1}{N} \sum_{l=0}^{L-1} g_l \sum_{m=1-N}^{N-1} C_{0,0}(m) R_h(d_\mu + mT_c - \tau_l) \quad (4)$$

$$R_S(d_\mu, d_\nu) = \frac{1}{N^2} \sum_{l=0}^{L-1} \sum_{q=0}^{L-1} g_l g_q^* \sum_{i=-\infty}^{\infty} \sum_{m=1-N}^{N-1} (N-|m|) R_h(d_\mu + mT_c - iT - \tau_l) R_h^*(d_\nu + mT_c - iT - \tau_q) \quad (5)$$

$$R_M(d_\mu, d_\nu) = \frac{1}{N^2} \sum_{l=0}^{L-1} \sum_{q=0}^{L-1} g_l g_q^* \sum_{i=-\infty}^{\infty} \sum_{m=1-N}^{N-1} (N-|m|) R_h(d_\mu + mT_c - iT - \tau_l) R_h^*(d_\nu + mT_c - iT - \tau_q) \delta_{i,m} \quad (6)$$

$$R_N(d_\mu, d_\nu) = \frac{1}{N} \sum_{m=1-N}^{N-1} C_{0,0}(m) R_h(d_\mu - d_\nu + mT_c) \quad (7)$$

where $\mu, \nu = 1..J$, g_l and τ_l are the complex channel coefficient and the delay of the l th resolvable multipath, respectively, parameter $\delta_{i,m}$ is unity except for the case $i = m = 0$, $R_h(t)$ is the autocorrelation function of $h(t)$ defined as

$$R_h(t) @ \int_{-\infty}^{\infty} h(t+\tau) h^*(\tau) d\tau \quad (8)$$

and

$$C_{k,i}(m) @ \begin{cases} \sum_{n=0}^{N-1+m} c_{k,i}(n-m) c_{0,0}^*(n), & 1-N \leq m < 0 \\ \sum_{n=0}^{N-1-m} c_{k,i}(n) c_{0,0}^*(n+m), & 0 \leq m \leq N-1 \\ 0, & \text{otherwise} \end{cases} \quad (9)$$

is the aperiodic cross-correlation function [18].

4. System Model and Assumptions

A downlink transmission scheme is considered. The information data are spread with Walsh codes and the chip sequences are QPSK modulated. In order to reduce ISI, the transmitted signal is low-pass filtered with a root-raised-cosine (RRC) pulse shaping filter with roll-off factor 0.22 in the frequency domain [19]. The transmitted signal of the k th user is

$$x_k(t) = \sqrt{\frac{E_k}{N}} \sum_{i=-\infty}^{\infty} s_{k,i} \sum_{j=0}^{N-1} c_{k,i}(j) h(t - iT - jT_c) \quad (10)$$

with $s_{k,i}$ the i th data symbol of the k th user.

In order to perform a fair comparison between our proposal and notable methods, channel parameters were taken as in [8]. Thus, we consider a time-invariant propagation channel with four resolvable multipaths. Table 1 gives the channel parameters, complex coefficients and delays, normalized to the ones of the strongest multipath. The delay of the first incoming multipath τ_0 is set equal to zero to account for synchronization. A perfect knowledge of channel state information (CSI) is further assumed (in practice, CSI is usually obtained by using pilot symbols or pilot channel(s) but it may also be estimated from the G-RAKE itself by comprising additional circuitry in the receiver [6,20]).

Table 1. Channel parameters.

l	$ g_l $ (dB)	$\arg(g_l)$ (rad)	$\tau_l (T_c)$
0	0	0	0
1	-1.5	$\pi/3$	1
2	-3.0	$2\pi/3$	2
3	-4.5	π	3

The incoming signal at the G-RAKE receiver front-end is

$$r(t) = \sum_{l=0}^{L-1} g_l \sum_{k=0}^K x_k(t - \tau_l) + n(t) \quad (11)$$

with $n(t)$ the intercell interference plus thermal noise component. The receiver, see Fig. 1, comprises J fingers, each correlating to a different received signal delay d_j , $j = 1..J$. Then, the fingers outputs are properly combined by using ML principles and form a decision statistic. The optimal receiver design problem is a $2J$ -dimensional one as long as both fingers positions and combining weights are

optimized. The first are heuristically found within a given search window so as to maximize the receiver gain (3), or equivalently the bit error rate (2), while the second are calculated from (1) by using the maximum likelihood criterion.

In this paper, we propose and evaluate three different finger placement strategies. In the first receiver design (it will be noted as G-RAKE_a), fingers are optimally set at integer multiples of the chip period while in the rest, fingers are fractionally spaced. In each case, the observation interval for the possible finger delays ranges from four chip prior to the earliest arriving multipath to four chips after the latest one; this search window is segmented in chip periods and in halves and tenths of the chip duration, respectively, for each scheme. Within this context, the fractionally spaced receivers will be noted as G-RAKE_b (fingers spacing is multiples of $T_c/2$) and G-RAKE_c (fingers spacing is multiples of $T_c/10$).

5. Numerical Results and Discussion

In this Section, we provide representative examples that demonstrate the performance of each design structure and highlight its potential advances in terms of throughput and complexity compared to methods in the literature. Unless otherwise stated, in the following examples, the processing gain is 128, the number of active users is 24 and the bit energy to power noise ratio is 10dB.

In Table II, we give the optimal fingers positions (normalized to T_c) for the proposed receivers with varied number of fingers. In the same Table, the calculated SNR values are presented. The conventional chip-spaced ML RAKE [7,17] in which the fingers are aligned with the resolvable multipaths (example #1) is also studied. For comparison reasons, we further consider the generalized RAKE receiver G-RAKE_a (#2) with a similar finger placement as before; in this J -dimensional optimization problem, only finger weights are optimally calculated.

Table 2. Receiver gain and finger placement of RAKE receivers.

#	Receiver type	SNR (dB)	Fingers positions (in T_c)							
			d_1	d_2	d_3	d_4	d_5	d_6	d_7	d_8
1	ML RAKE	3.06	0	1	2	3	-	-	-	-
2		3.50	0	1	2	3	-	-	-	-
3		5.49	-1	0	-	-	-	-	-	-
4	G-RAKE_a	6.39	-1	0	1	-	-	-	-	-
5		6.60	-1	0	1	2	-	-	-	-
6		6.77	-1	0	1	2	3	-	-	-
7		4.52	0.5	0	-	-	-	-	-	-
8		5.77	-1	0.5	0	-	-	-	-	-
9		6.09	-1	0.5	0	0.5	-	-	-	-
10	G-RAKE_b	6.65	-1	0.5	0	0.5	1	-	-	-
11		6.73	-1	0.5	0	0.5	1	1.5	-	-
12		6.97	0.5	0	0.5	1	1.5	2	2.5	-
13		7.12	0.5	0	0.5	1	1.5	2	2.5	3
14	G-RAKE_c	5.78	1.1	0.1	-	-	-	-	-	-
15		6.59	1.1	0.1	1.4	-	-	-	-	-

In contrast to the MRC RAKE and the G-RAKE_a (#2), the optimal finger placement sets one or more fingers earlier

to the first arriving multipath to suppress interference. The specific finger placement leads to a partial cancellation of the overall noise because the noise on the added finger(s) is correlated to the noise on the rest. This allocation, in combination with the advanced calculation of the combining weights, increases the receiver gain compared to the ML RAKE and the G-RAKE_a (#2), even for structures with less fingers. The enhanced performance of the G-RAKE_c receivers compared to the rest of the structures with the same number of fingers is also shown. We further notice that by placing extra fingers to collect signal energy the SNR increases but this improvement gradually reduces with J . The improved performance of the G-RAKE compared to the ML RAKE with the same number of fingers and finger positions (examples #2 and #1, respectively) is due to improved calculation of the combining weights (the G-RAKE further accounts for different noise level on the fingers and noise correlation between them). It has to be noticed that in our study, the multipath rays are chip-spaced, see Table 1; as a result, the G-RAKE_a fingers are aligned with the received multipaths and/or positioned at the strongest paths of the inverse channel filter. If this is not a case, it is expected that the G-RAKE_a performance degrades.

Next, a detailed study of a representative set of G-RAKE receiver structures is performed. In particular, in Figs. 2-7, we evaluate the performance of the G-RAKE_a (#2, #4, #5, #6), G-RAKE_b (#10) and G-RAKE_c (#15) receivers. In each figure, the performance of the four-finger conventional MRC RAKE [6,7] is also depicted for comparison reasons; in this structure, the chip-spaced fingers are aligned with the incoming multipaths.

Figure 2 shows the bit error rate performance of the aforementioned receivers. Notice that even the G-RAKE_a with four fingers aligned with the multipaths, outperforms the conventional MRC RAKE due to the optimization of fingers weights (a similar performance was noticed in [8]). Moreover, by setting a finger on the strongest tap of the inverse channel response, system performance improves noticeably demonstrating the tradeoff between signal energy collection and noise whitening. On the other hand, when we place extra fingers to collect signal energy, system performance does not improve significantly. As it has already been mention, the incoming multipaths are chip-spaced; if this not a case, a superior performance of G-RAKE_c compared to the rest of the G-RAKE implementations is expected.

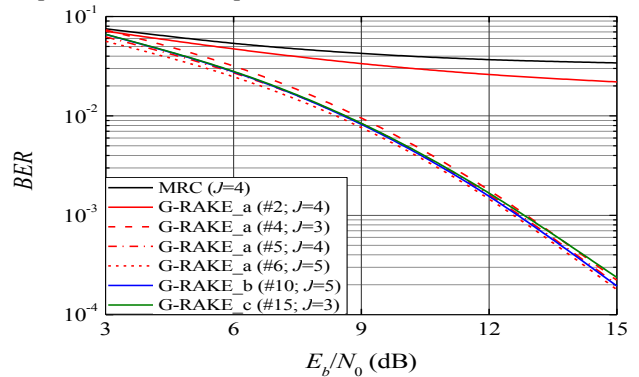


Fig. 2. Bit error rate curves for the MRC RAKE and representative suboptimal G-RAKE receivers ($K = 24; N = 128$).

Similar results are obtained from the study of system capacity in terms of maximum active users (traffic load), see

Fig. 3. In this figure, the bit error rate is depicted as a function of K for bit energy to power noise ratio values equal to 9 and 15dB. We further notice that the improvement in system performance due to noise whitening and interference suppression as a result of the positioning of one or more fingers before the earliest arriving multipath increases with E_b/N_0 . Moreover, the slope of the BER curves decreases with K which implies that the variations in the number of active users have a more severe impact on system performance at lower traffic loads.

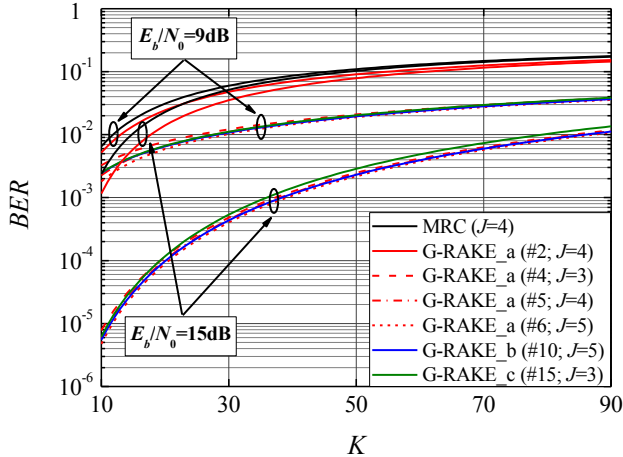


Fig. 3. Bit error rate versus K for the MRC RAKE and representative suboptimal G-RAKE receivers ($N = 128$).

Interesting results for the impact of the bit energy to power noise ratio on the maximum number of active users are obtained from Fig. 4 that shows K versus E_b/N_0 for maximum bit error rates 10^{-2} , 10^{-3} and 10^{-4} . In the MRC and G-RAKE_a (#2) receivers, the maximum number of users allowed slightly increases with E_b/N_0 . However, the rest of the structures show an enhanced performance due to the sophisticated fingers placement; in these implementations, K depends strongly on E_b/N_0 while the increase in capacity is more pronounced at lower E_b/N_0 values. In all scenarios, an upper bound in the maximum number of users is observed at high E_b/N_0 . In this case, MUI is dominant among the total interference (interference limited system) and any further increase in signal energy would no longer be beneficial [21].

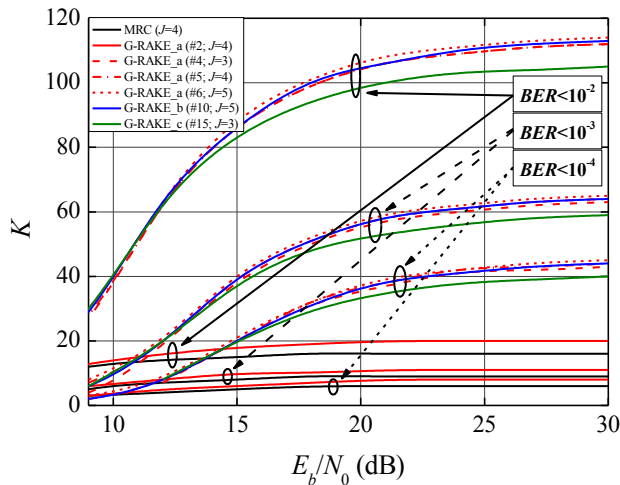


Fig. 4. Maximum number of active users versus E_b/N_0 for the MRC RAKE and representative suboptimal G-RAKE receivers ($N = 128$).

In the next two examples, we explore the relation between system performance and processing gain. Figure 5

shows the impact of the processing gain on BER performance for the RAKE receivers previously studied. Clearly, the bit error rate decreases with N as it can easily be explained from (3)-(7); in particular, the desired signal component does not depend on N whereas the elements of the \mathbf{R}_s , \mathbf{R}_M and \mathbf{R}_N matrices reduce with processing gain (in general, in the presence of wide-sense stationary uncorrelated scattering (WSSUS) fading [22], the MUI and ISI correlation coefficients between the signals at the fingers outputs of a RAKE receiver decrease with N while the desired signal correlation coefficients does not depend on it [23]). These further explain the advanced performance for high N values, of the MRC RAKE and G-RAKE_a (#2) compared to the rest of the G-RAKE implementations with the same number of fingers. The first two receivers use all their fingers for signal collection (recall that, the desired signal component does not depend on the processing gain); on the other hand, the rest of the structures use one or more fingers for suppressing interference, which reduces with N . At this point, we should remind that in the implementations presented in Table 2, fingers optimal positions were calculated for $N = 128$; obviously, an optimization performed for different values of N would give structures with better or at least the same performance with G-RAKES with the same number of fingers aligned at the incoming multipaths. The previous discussion also explains the advanced performance of the G-RAKE_a receivers with four and five fingers compared to the G-RAKE_b with $J = 5$ (the first two implementations use one finger for interference suppression and the rest of them for signal collection, while the G-RAKE_b (#10) uses two of its fingers for interference suppression).

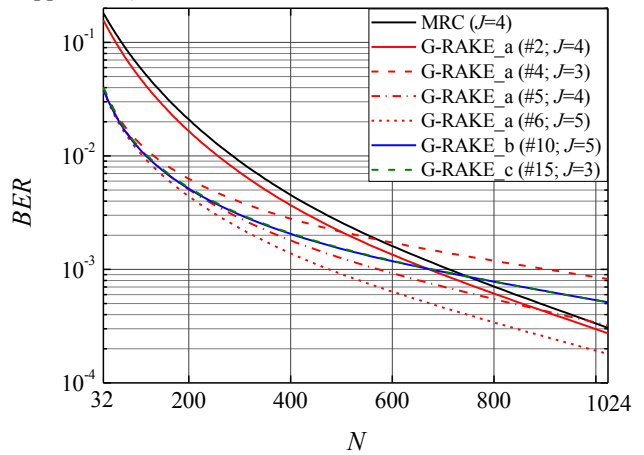


Fig. 5. Impact of processing gain on system performance in terms of bit error rate for the MRC RAKE and representative suboptimal G-RAKE receivers ($K = 24$; $E_b/N_0 = 9$ dB).

The relation between K and N is depicted in Fig. 6. The illustrated curves show the maximum number of users that are allowed for bit error rates less than 10^{-2} and 10^{-3} and bit energy to power noise ratio $E_b/N_0 = 15$ and 21dB. As it was expected, K increases with E_b/N_0 and the maximum acceptable bit error rate. Notice also that the maximum number of allowed users is practically proportional to N verifying the outcomes of earlier studies in the published literature³. As it has already been commented in the previous paragraph, the improved performance of the G-RAKE_a (#4)

³ The number of users which can be handled from a RAKE receiver that operates in an ISI-free WSSUS channel is proportional to the processing gain [21,23].

compared to the G-RAKE_a (#5) and (#6) and the poor performance of the G-RAKE_c is due to the fact that the fingers positions were calculated so as to optimize system performance for a processing gain equal to 128.

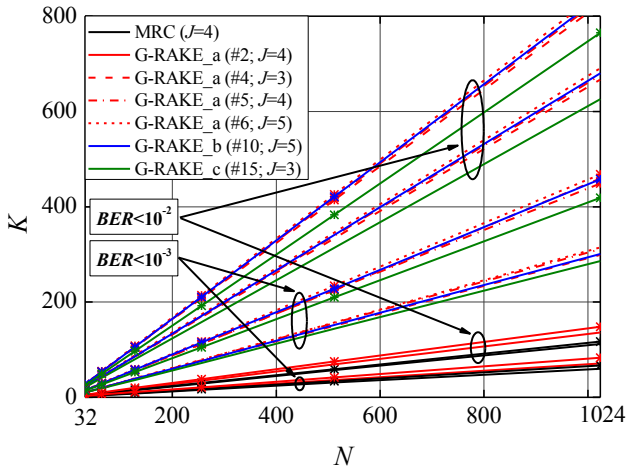


Fig. 6. Impact of processing gain on the maximum number of active users for the MRC RAKE and representative suboptimal G-RAKE receivers; E_b/N_0 is equal to 15dB (“”) and 21dB (“*”).

In the previous examples, we considered a four-ray, chip-spaced channel with parameters given in Table I. In Table III, we present the (normalized to the chip period) optimal finger delay positions in G-RAKE_b structures with J that varies from 2 to 8 (examples #7 to #13) and G-RAKE_c implementations with $J = 2$ and 3 (examples #14 and #15, respectively) when the channel comprises the first two or three multipath components only (two- and three-ray channels). In order to improve the clarity of the exposition, the optimum finger settings for the four-ray channel are also given. The analysis of the obtained results provides some interesting conclusions. First of all, the J th finger moves towards to greater values with L so as to compensate for the increase in channel spread and collect the additional signal energy [24]. However, in most of the cases, the earlier fingers are set closer to the first arriving multipath for noise whitening and interference suppression (this is a significant difference with several finger allocation strategies in the published literature, e.g. [7,21,24,25]; in these cases, all the fingers move towards greater delays when channel spread increases). Notice also that the changes in channel spread have a stronger impact on the fingers with greater delays (a similar performance is observed in several optimum finger assignment schemes in the literature, e.g. [21].) In any case, the range of the fingers delays, that is, the difference $y(d_j) - y(d_1)$, increases with channel spread.

Table 3. Optimal finger placement in representative G-RAKES for $L = 2/3/4$.

#	Receiver type	Fingers positions (in T_c)							
		d_1	d_2	d_3	d_4	d_5	d_6	d_7	d_8
7	G-RAKE_b	0/							
		-							
		0.							
		5/	0.5/0/						
		-	0						
8	G-RAKE_b	0.							
		5/	0/0/-	0.5/0.					
		-	0.5	5/0					
		0.							
		5/							

9	G-RAKE_c	-1							
		-							
		0.							
		5/	0/0/-	0.5/0.	1/1/0				
		-	0.5	5/0	.5				
		0.							
		5/							
		-							
		0.							
		5/	0/0/-	0.5/0.	1/1/0	1.5/1.			
10	G-RAKE_c	-							
		0.							
		5/	0/0/-	0.5/0.	1/1/0	1.5/1.			
		-	0.5	5/0	.5	5/1			
		0.							
		5/							
		-							
		0.							
		5/							
		-							
11	G-RAKE_c	1/							
		-							
		0.							
		5/	0.5/0/	0/0.5/	0.5/1	1/1.5/	1.5/2		
		-	-0.5	0	/0.5	1	/1.5		
		0.							
		5/							
		-							
		0.							
		5/							
12	G-RAKE_c	-							
		1.							
		5/							
		-							
		0.							
		5/							
		-							
		0.							
		5/							
		-							
13	G-RAKE_c	1.							
		5/							
		-							
		0.							
		5/							
		-							
		0.							
		5/							
		-							
		0.							
14	G-RAKE_c	1/							
		-							
		0.							
		5/	1/0.2/						
		-	0.1						
		0.							
		5/							
		-							
		0.							
		5/							
15	G-RAKE_c	6/							
		-							
		0.							
		5/							
		-							
		0.							
		5/							
		-							
		0.							
		5/							

In order to further investigate the impact of channel spread on system performance, we calculate the receiver gain of a plurality of receivers that operate in environments with varied channel spread. Figure 7 depicts the calculated SNRs for a set of G-RAKE_b and G-RAKE_c receivers and channels with two, three and four rays and parameters given in Table I. The fingers positions are given in Table II. Clearly, SNR reduces with channel spread due to the increased energy spread and the higher level of interference which results from the greater number of incoming signal components. Moreover, performance degradation gradually diminishes with the increase of incoming multipaths. More comparisons (not presented here) between G-RAKES and conventional RAKE structures have shown that the performance degradation due to channel spread is smaller to the first exhibiting that the necessity to perform noise coloration increases with channel spread; see, also, [8].

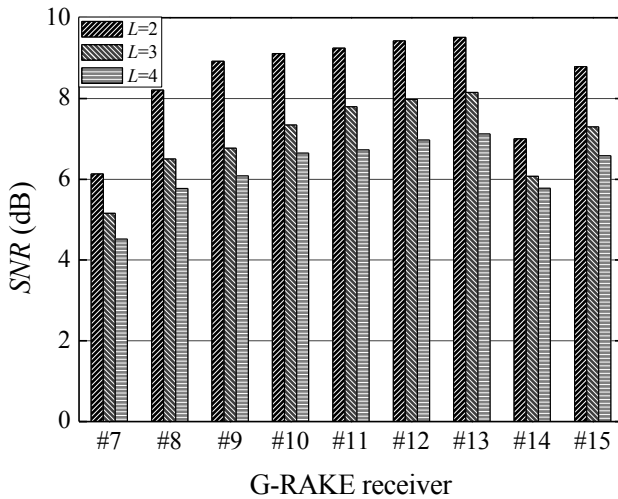


Fig. 7. G-RAKEs receiver gain versus channel spread ($K = 24$; $N = 128$; $E_b/N_0 = 10\text{dB}$).

Our analysis has shown that the proposed G-RAKEs show an enhanced performance compared to conventional structures such as the MRC and the ML RAKE receiver. Clearly, the placement of one or more fingers before the earliest arriving multipath improves system performance by suppressing interference at the extent that G-RAKEs outperform structures with greater number of fingers in which conventional finger allocation schemes are followed. The sophisticated calculation of fingers positions and weights further improves receiver performance. Moreover, fractionally finger spacing provides us with receivers with similar performance at lower complexity or improved performance at higher complexity compared to chip-spaced implementations. In earlier analyses, e.g. [8], fingers were placed with an almost infinite time resolution. However, in practice, the resolution of finger placement in a receiver is limited by sampling interval, which is usually a few fraction of the chip duration [21]. Thus, the G-RAKE_b and G-

RAKE_c structures (esp. the second one, due to its improved performance) can be easily considered as serious candidates for real DS-CDMA wireless communication systems.

6. Conclusions

In this paper, we proposed three maximum likelihood G-RAKE receivers with suboptimal finger placement and analyzed their performance in terms of bit error rate and capacity. In the proposed implementations, fingers are optimally placed at integers or at fractions of the chip period while their weights are calculated by using ML principles so as to increase the receiver gain. Besides, a set of the fingers are placed before the first arriving multipath so as to cancel the noise coloration caused by the channel and suppress interference. Representative examples indicated the enhanced performance of the proposed receivers compared to the conventional MRC and ML RAKE with greater hardware complexity while the sophisticated placement of the fingers allows the design of even simpler G-RAKE structures. Within this context, a series of other interesting conclusions were also drawn. It was found that system performance improves with the number of RAKE fingers but this improvement gradually diminishes as this number increases. The spread of the propagation medium affects noticeably both finger optimal positions and system performance. The last degrades with channel spread but the degradation gradually reduces with the number of resolvable multipaths. The processing gain has a severe impact on system performance in terms of bit error rate and traffic load, esp. at high bit energy to power noise ratio values. An increase in the processing gain reduces significantly the bit error rate and increases linearly the maximum allowed number of users. Finally, the variations in the number of active users have a more severe impact on system performance at lower traffic loads while an upper threshold limits their maximum number.

References

- Javaid, U., Rasheed, T., Meddour, D.-E., Ahmed, T., and Prasad, N.R., "A novel dimension of cooperation in 4G", IEEE Technology and Society Magazine, Vol. 27, No. 1, pp. 29-40, (2008).
- Mahmood, A., "Cooperative diversity in wireless networks", Journal of Engineering Science and Technology Review, Vol. 3, No. 1, pp. 184-187, (2010).
- Holma, H., and Toskala, A. (Eds.), WCDMA for UMTS – HSPA Evolution and LTE, 5th ed., John Wiley & Sons, New York, (2011).
- Mousa, A., "Electromagnetic radiation measurements and safety issues of some cellular base stations in Nabus", Journal of Engineering Science and Technology Review, Vol. 4, No. 1, pp. 35-42, (2011).
- Ekpenyong, M.E., Eromosele, G., and Isabona, J. "On the performance modeling of outage probability in CDMA wireless networks", Journal of Engineering Science and Technology Review, Vol. 4, No. 2, pp. 174-182, (2011).
- Baltzis, K.B. "The rake receiver principle: Past, present and future", Recent Patents on Electrical Engineering, Vol. 5, No. 1, pp. 55-71, (2012).
- Lee, J.S., and Miller, L.E., CDMA Systems Engineering Handbook, Artech House, Boston, (1998).
- Bottomley, G.E., Ottoson, T., and Wang, Y.-P.E., "A generalized RAKE receiver for interference suppression", IEEE Journal of Selected Areas in Communications, Vol. 18, No. 8, pp. 1536-1545, (2000).
- Bottomley, G.E., Cairns, D.A., Cozzo, C., Fulghum, T.L., Khayrallah, A.S., Lindel, P. *et al.*, "Advanced receivers for WCDMA terminal platforms and base stations", Ericsson Review, Vol. 8, No. 2, pp. 54-58, 2006.
- Fulghum, T., Cairns, D.A., Cozzo, C., Wang, Y.-P.E., and Bottomley, G., "Adaptive generalized rake reception in DS-CDMA systems", IEEE Transactions on Wireless Communications, Vol. 8, No. 7, pp. 3464-3474, (2009).
- www.ericsson.com
- Baltzis, K.B., "An efficient finger allocation method for the maximum likelihood RAKE receiver", Radioengineering, Vol. 17, No. 4, pp. 45-50, (2008).
- He, J., and Salehi, M., "A new finger placement algorithm for the generalized RAKE receiver", Proceedings of the 42nd Annual Conference on Information Sciences and Systems, Princeton, USA, pp. 335-340, (2008).
- Thomos, C., Papadopoulos, C., and Kalivas, G., "Design and implementation of a low-complexity RAKE receiver and channel estimator for DS-UWB", Proceedings of the

- 15th IEEE Mediterranean Electrotechnical Conference, Valletta, Malta, pp. 93-98, (2010).
15. Baltzis, K.B., and Sahalos, J.N., "Suboptimal RAKE finger allocation: Performance and complexity tradeoffs", *Journal of Electrical Engineering*, Vol. 61, No. 2, pp. 107-113, (2010).
 16. Meles, E.S., and Baltzis, K.B., "Design, analysis and optimization of a fractionally spaced maximum likelihood G-RAKE receiver", *Proceedings of the 2nd Pan-Hellenic Conference on Electronics and Telecommunications*, Thessaloniki, Greece, pp. 1-4, (2012).
 17. Proakis, J., and Salehi, M., *Digital Communications*, 5th ed., McGraw-Hill, New York, (2008).
 18. Pursley, M.B., Sarwate, D.V., and Stark, W.E., "Error probability for direct-sequence spread-spectrum multiple-access communications—Part I: Upper and lower bounds", *IEEE Transactions on Communications*, Vol. 30, No. 5, pp. 975-984, (1982).
 19. Dahlman, E., Beming, P., Knutsson, J., Ovesjö, F., Persson, M., and Roobol, C., "WCDMA-the radio interface for future mobile multimedia communications", *IEEE Transactions on Vehicular Technology*, Vol. 47, No. 4, pp. 1105-1118, (1998).
 20. Cairns, D.A., "Convolutional impairment covariance estimation method and apparatus", US Patent Application 20110014874, (2011).
 21. Baltzis, K.B., and Sahalos, J.N., "A novel RAKE receiver design for wideband wireless communications", *Wireless Personal Communications*, Vol. 43, No. 4, pp. 1603-1624, (2007).
 22. Jeruchim, M.C., Balaban, P., and Shanmugan, K.S., 2nd ed., *Kluwer Academic/Plenum Publishers*, New York, (2000).
 23. Baltzis, K.B., "Impact of finger placement on the correlation properties of rake combined signals", *Radioengineering*, Vol. 18, No. 4, pp. 469-476, (2009).
 24. Kim, K.J., Kwon, S.Y., Hong, E.K., and Whang, K.C., "Effect of tap spacing on the performance of direct-sequence spread-spectrum RAKE receiver", *IEEE Transactions on Communications*, Vol. 48, No. 6, pp. 1029-1036, (2000).
 25. Li, C.-M., and Li, H.-J., "A novel RAKE receiver finger number decision rule", *IEEE Antennas and Wireless Propagation Letters*, Vol. 2, pp. 277-280, (2003).